DEVICE-LAYER OVENIZATION OF FUSED SILICA MICROMECHANICAL RESONATORS FOR TEMPERATURE-STABLE OPERATION

Zhengzheng Wu[*]*, Adam Peczalski, and Mina Rais-Zadeh*
University of Michigan, Ann Arbor, MI 48109, USA

ABSTRACT

In this paper, we report on temperature-stable operation of multiple MEMS silica resonators on an ovenized fused silica device-layer. Temperature servo-control circuits are implemented for compensating the resonator frequency drift using an on-chip RTD-based temperature sensor. A wide linear range analog controller has been implemented to reduce the effective TCF of fused silica resonator by an order of magnitude. Digital calibration method is further proposed and characterized to mitigate the offset errors induced from the non-ideal temperature sensing. Calibration reduces the resonator frequency drift to within 5 ppm across 105 °C of external temperature change. The power consumption of the ovenized device-layer is lower than 16.2 mW.

INTRODUCTION

Towards the ultimate goal of realizing a silica-based integrated timing and inertial measurement unit (TIMU), high-performance micro-electromechanical resonators [1], silica packaging processes, and multi-layer vertically stacked fused silica microsystems [2] have been demonstrated. Such technologies leverage material properties of fused silica to realize both resonant MEMS devices and hermetic packages for multi-sensor platforms. In terms of thermal properties of fused silica, a distinctive feature is its extremely low thermal conductivity of 1.3 W/m•K. However, due to a high temperature coefficient of elasticity (TCE) of ~+180ppm/K, fused silica TIMU requires temperature compensation techniques for stable operation. In this work, we take advantage of the low thermal conductivity to ovenize a large silica device layer with multiple micro-devices at low power levels. We further analyze the thermal design of the fused silica platform and present circuits for realizing closed-loop temperature control. The ovenized silica platform drastically improves temperature stability of silica MEMS resonators in the device fusion platform.

OVENIZED FUSED SILICA DEVICE-LAYER

It has been reported that fused silica MEMS resonators exhibit a high temperature coefficient of frequency (TCF) of ~ +89 ppm/K [1]. The high TCF is mostly attributed to the high temperature TCE of the fused silica material. While passive material compensation has been employed to reduce the TCF of MEMS resonators [3], the high TCE of fused silica makes passive compensation difficult. On the other hand, ovenization is known to offer excellent thermal stability. Ovenized quartz crystal oscillators (OCXOs) are known to deliver best stability among crystal timing references. Moreover, ovenized MEMS resonators have been demonstrated with power consumption as low as tens of milli-Watts [4]. However, most reported approaches are specific to a single resonator and are not directly applicable to a multi-device system such as the TIMU sensor fusion platform.

In this work, we demonstrate an ovenized fused silica layer (or platform) that can stabilize multiple MEMS devices over a wide external temperature range. The platform active area is 3.5 mm× 3.5 mm and includes four MEMS resonators. A scanning electron microscope (SEM) image of the fabricated fused silica platform is shown in Fig. 1. A resistance temperature detector (RTD) is co-fabricated on the silica device-layer using a 1000 Å-thick platinum (Pt). The RTD has a nominal resistance of 7 kΩ. A Pt

heater ring is placed on the edge of the active area and can be used to heat the platform to a fixed oven set temperature.
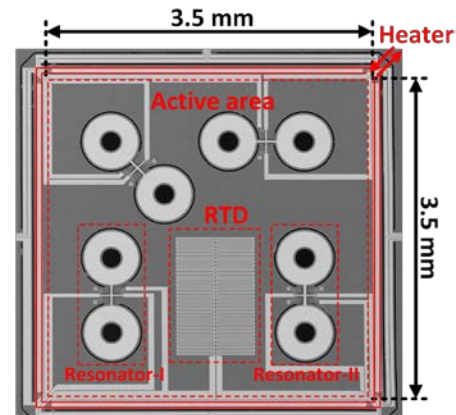

Figure 1: SEM image of a fused silica platform consisting of four resonators, an integrated RTD, a heater, and thermal isolation legs.

In order to reduce the power consumption, it is critical to thermally isolate the active area from the external environment. Heat transfer mechanisms from a MEMS device to external environment include heat conduction, heat convection, and radiation heat transfer. For minimizing heat conduction transfer, design of thermal isolation structures is critical. As shown in Fig. 1, the active area is connected to the external boundary using thermal isolation legs. With the low thermal conductivity provided by fused silica, eight thermal isolation legs with relatively large width (100 μm) are used. Such a design improves robustness by avoiding long and meandered supporting legs used in silicon MEMS [4], while good thermal isolation is still maintained. Also, the wide legs allow wiring of multiple low-resistance electrical connections to external pads using a thin-film metal layer, which favor integrating multiple devices on the platform. Using COMSOL FEM simulation, the thermal resistance of the designed isolation structure is extracted to be 28 K/W if heat conduction through solid structures dominates heat transfer (Fig. 2). Additional challenges arise in developing a large ovenized MEMS device-layer as compared to an individual MEMS device. Due to a larger surface area, the heat loss is more susceptible to convection and radiation heat transfer. When a high vacuum condition (pressure lower than 1 mTorr) cannot be obtained, the assumption that heat conduction dominates heat transfer is no longer valid. As a result, the effective thermal resistance decreases. Heat losses from convection and radiation are further included in the FEM simulation studies. To take into account for typical vacuum condition in a hermetic MEMS package, a heat transfer coefficient (*h*) of 0.05 W/m2•K is assumed for modeling the convection heat loss, which amounts to mTorr pressure level typically seen in a MEMS package. The radiation effect is simulated as surface-to-ambient radiation with surface emissivity of 0.9, accounting for the material property of fused silica. With an ambient temperature of 233 K (-40 °C), the temperature increase at the center of the silica active area relative to ambient is simulated as a function of the heating power, and results are also plotted in Fig. 2. It can be seen that the effective thermal resistance is reduced

(indicating worse thermal isolation) by more than four times compared to the results that only consider conduction heat transfer.
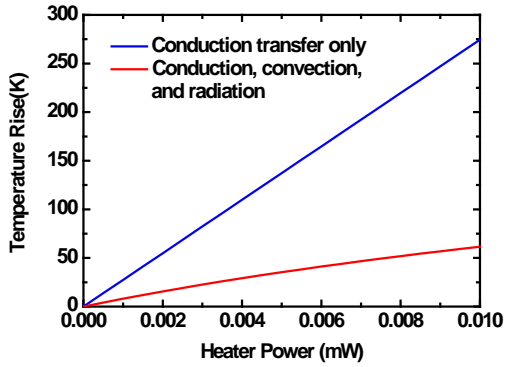

Figure 2: Temperature rise of the fused silica device-layer versus heater power from COMSOL FEM simulation.
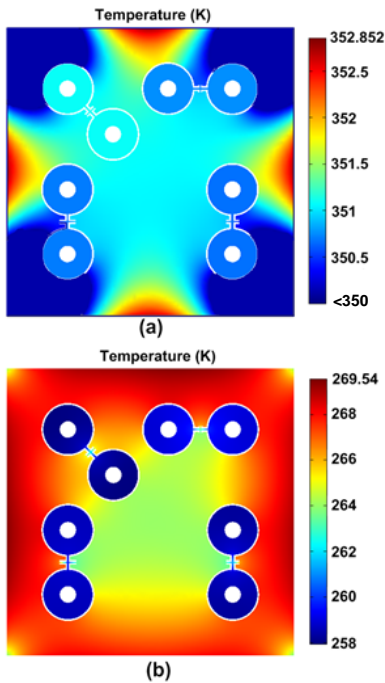

Figure 3: Temperature distribution within the active area when 4.3 mW of power is applied to the heater at an external temperature of 233 K: (a) only considering conduction heat transfer; (b) considering heat conduction, convection, and radiation.

Moreover, there exists larger temperature non-uniformity across the active area due to heat loss from heat convection and radiation. Figure 3 shows the temperature distribution within the fused silica active area when a heater power of 4.3 mW is applied to heat up the device to oppose an external temperature of 233 K (-40 °C). Figure 3(a) only considers conduction heat transfer. It can be observed that temperature across the large active area is quite uniform. The four devices on the platform show less than 1 K of temperature difference. Figure 3(b) includes the effect of convection and radiation heat transfer. It can be found that a much larger temperature gradient exists inside the active area. As high-Q MEMS resonators typically use long and narrow tethers to reduce anchor loss [1]; the large thermal resistance inherent in these tethers

causes a large temperature gradient from the resonator bodies to the anchor area when the resonator bodies loose heat due to convection and radiation. As a result, the resonators experience large temperature offsets compared to the region where the RTD is placed. Therefore, it is very challenging for the RTD to accurately sense the real temperature of MEMS devices.

TEMPERATURE CONTROLLER DESIGN
High Gain Analog Controller

An analog servo-control system is implemented for monitoring the RTD response and generating a feedback power control signal. As shown in the circuit schematic in Fig. 4, the RTD is connected in a Wheatstone bridge configuration along with three other low-TCR and precision resistors. The Wheatstone bridge is interfaced to an instrumentation amplifier (IA) for pre-amplification. The IA provides a high voltage gain of 10,000 and ensures that temperature is measured with a low offset error. The signal generated from the IA is filtered and fed to a heater driver stage. The heater driver is implemented using an analog square-root generator based on BJT translinear circuits [5]. The square-root generator linearizes the transfer function from the input control voltage to the output heater power. Figure 5 plots the normalized power gain versus input voltage of the square-root generator extracted from measurement. Compared to an earlier work that employed a linear amplifier to generate a heater current proportional to the sensor signal [6], the heater driver design in this work performs linearization and ensures a near constant thermal loop gain across a wide input range (Fig. 5). Therefore, a sufficient power gain can be ensured even at low heater power levels. Using this heater driver, the oven temperature can be set close to the maximum device working temperature without degrading the control performance, thus minimizing the power consumption of ovenization.
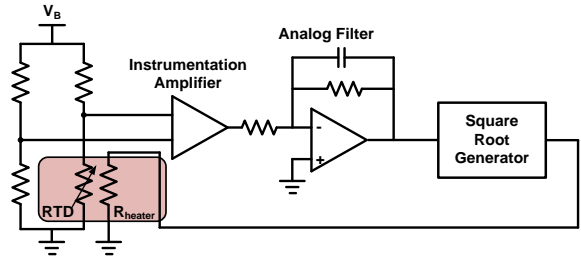

Figure 4: Circuit schematic of the resistive temperature detector (RTD) interface and analog oven-control system.
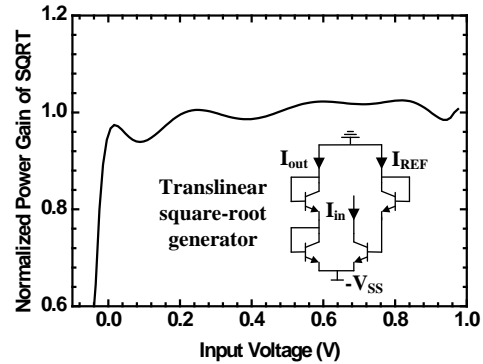

Figure 5: Normalized power gain versus input voltage of the square-root generator (with translinear square-root circuit schematic inset).

The temperature stability of a MEMS resonator inside the active area is measured over external temperature changes. Before taking measurements, the bulk micromachined fused silica die is mounted on a silicon carrier attached to a ceramic package (Fig. 6). The signal pads are bondwired to the ceramic package for external electrical connections. Thermal conductive glue is used to ensure good thermal conductivity between interfaces. During temperature measurements, the whole package is placed in a vacuum chamber. The vacuum chamber maintains a vacuum level of less than 10 mTorr, and the temperature can be set to different values with +/-0.1 K of accuracy. While the analog temperature controller is used to provide a servo-control, the frequency drift of the MEMS resonator is monitored using a network analyzer. The frequency drift of Resonator I (in Fig. 1) over a chamber temperature from -40 °C to +75 °C is plotted in Fig. 7. Using oven-control, the effective TCF of the fused silica resonator has been reduced to +10 ppm/K, as compared to +89 ppm/K for an uncompensated silica resonator.

The effective thermal loop gain of the analog controller has been extracted to be as high as ~1900. Although the active compensation has reduced the uncompensated TCF of a fused silica resonator by almost an order of magnitude, a significantly smaller drift is expected due to a large thermal loop gain provided by the servo-control system. Yet, there is overall frequency drift of 1163 ppm over -40 °C to +75 °C. This is mainly due to the temperature gradient within the active area as analyzed in the previous section. Since the temperature sensor (RTD) is not sensing the true resonator temperature, further increasing the thermal loop gain is ineffective in improving the temperature control accuracy, as demonstrated with a loop gain of ~5,000 in Fig. 7. Such non-ideal property of resistive temperature sensor is especially pronounced for an ovenized fused silica active device-layer.
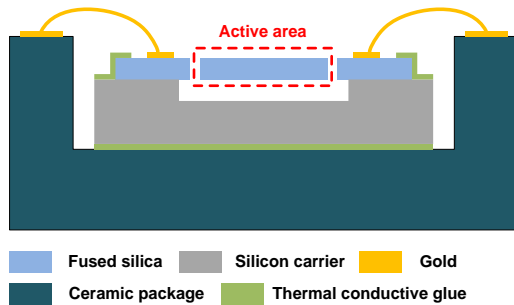

Figure 6: Cross-sectional view showing the fused silica die mounted in a ceramic package for temperature stability measurement.
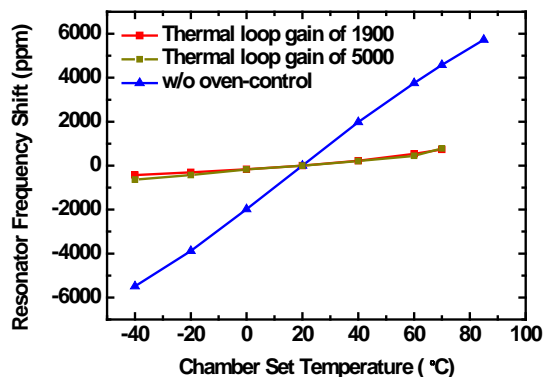

Figure 7: Measured frequency drift of Resonator I with analog control and TCF of a similar but uncompensated silica resonator.

Stability Improvement with Digital Calibration

In order to improve the temperature sensing accuracy, it is desirable to place the RTD sensor very close to the MEMS resonator or even on the resonator body. In this scenario, the temperature sensor readout will reflect the real device temperature with better fidelity. However, in order to design an RTD with sufficiently strong voltage output and minimal self-heating in a Wheatstone bridge configuration, an RTD needs to have large enough nominal resistance (typically kΩ range). To satisfy these requirements, the on-chip integrated RTD in this work occupies an area of approximately 1 mm^2. Although there is still room to shrink the footprint of the RTD, it is in general very difficult to place the RTD on the body of a MEMS resonator or a resonant sensor. Moreover, temperature compensation needs to be performed for all the devices in the device fusion platform, further complicating the design.

Considering the adverse effect of temperature gradient across the active area discussed in the previous section, the RTD-based temperature compensation method mainly suffers from offset errors due to a non-uniform temperature distribution. The offset error can be compensated using digital calibration in the temperature controller design. As plotted in Fig. 8, after the RTD sensor response is pre-amplified and filtered, the output voltage can be digitized for further processing. A digital calibration table is used to store the offset errors across the RTD sensor output range. After the data is converted back to analog domain to generate a heater control signal, the offset errors are effectively removed in the servo-control system. In order to maintain a constant loop gain, the square root function from control voltage to heater driver voltage can also be performed in a digital calibration look-up table to simplify the analog implementation.
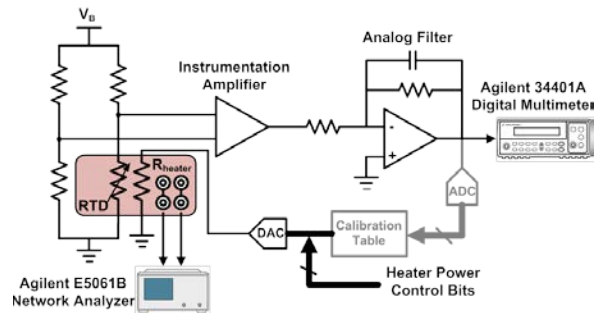

Figure 8: Circuit schematic of the RTD interface and oven-control system with digital calibration to reduce sensor offset.

To study the effectiveness of digital calibration in this work, the temperature control system is characterized by setting the control bits (instead of using a closed-loop operation) to control heater power according to different conditions. In the meantime, the output voltage from the RTD front-end (RTD with an IA and an analog filter) is monitored using a digital multimeter (Fig. 8). From the sensor output voltage measurement, the resistance change of the RTD can be back calculated. The frequencies of two MEMS resonators (Resonator I and Resonator II in Fig. 1) in the fused silica platform are also monitored using a Network Analyzer. The oven set temperature point is ~ 70 °C. At this oven set point, the RTD sensor front-end voltage output is adjusted to near zero.

In the first measurement setup, the RTD voltage output is maintained at zero output (constant RTD resistance) by the system across the chamber set temperature range. This is comparable to an analog controller with an integrator in the loop that keeps the RTD at a constant temperature. The frequency shift of two resonators are measured and plotted in Fig. 9. It is shown that although the RTD

sensor maintains a near constant temperature (within 0.04% of resistance change) through controlled heater power, the two resonators still exhibit obvious residue frequency shift. Resonator I experiences a total shift of 944 ppm, whereas resonator II shows a total shift of 697 ppm across a chamber set temperature range of -40 °C to +65 °C. It can be observed that Resonator I exhibits larger frequency drift than Resonator II. This is believed to mainly arise from the difference in the tether length of these two fused silica resonators. The support tethers of Resonator I is 90 μm in length as whereas Resonator II has 65 μm-long tethers. A longer tether will introduce a larger thermal resistance from the resonator body to the outer fused silica active area, making it harder to equalize the temperature with the external boundary. Placement of two resonators also slightly affects their temperature drifts.
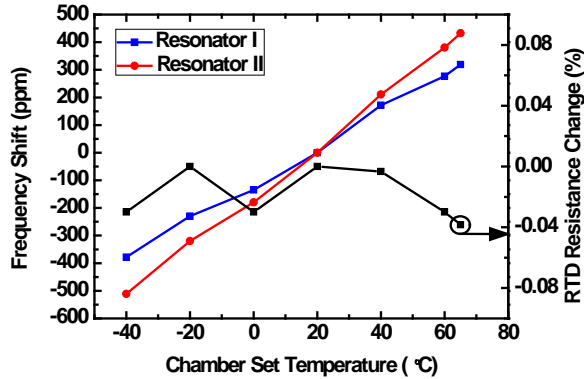

Figure 9: Frequency drift of two resonators with digitally controlled heater power to maintain a near constant RTD resistance (RTD resistance is included).

In the second measurement, the heater power is calibrated to stabilize the frequency of Resonator I. In this case, the frequency shift of two resonators are measured and plotted in Fig. 10. Benefited from calibration, the total frequency drift of Resonator I is less than 5 ppm. The total frequency drift of Resonator II is also improved to be within 264 ppm over the chamber set temperature of -20 °C to +65 °C. The output voltage from the RTD front-end is also monitored, and the extracted RTD resistance change is plotted in Fig. 10. It can be observed that the RTD is experiencing temperature increase at lower chamber temperatures if the system tries to stabilize the resonator frequency.
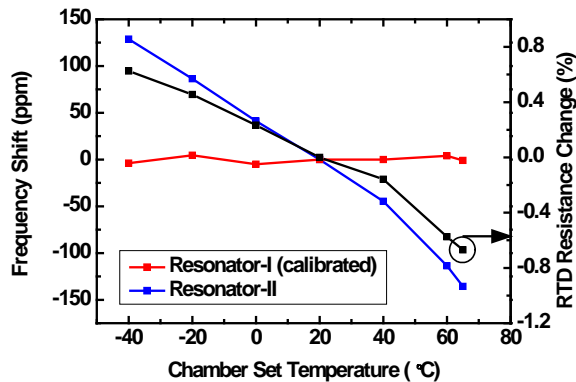

Figure 10: Frequency drift of two resonators with digitally controlled heater power to maintain a stable frequency for Resonator I (RTD resistance is included).

The power consumption of the heater is plotted and compared in Fig. 11 for the above two calibration settings. Due to the temperature difference between Resonator I and the RTD, a small amount of excessive heater power is needed to stabilize the frequency of resonators compared to maintaining a constant RTD resistance. The digital calibration method mentioned above can set the offset to achieve a constant frequency output. Benefited from low thermal conductivity of fused silica material, the power consumption of the ovenized device is less 16.2 mW across a wide external temperature range.
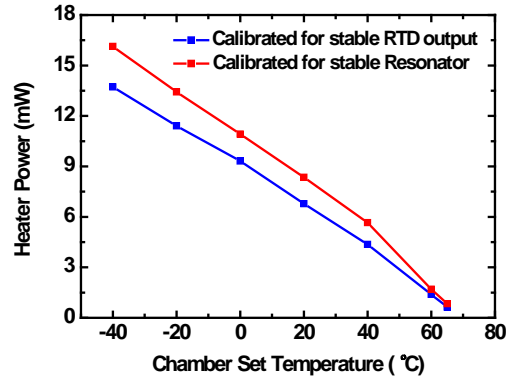

Figure 11: Extracted power consumption of the heater vs. chamber temperature.

CONCLUSION

In this work, a fused silica platform is implemented for integrating multiple MEMS devices on a single die. Thermal properties of the platform are analyzed, showing that the temperature of devices can be stabilized at low oven power levels. Temperature sensing and closed-loop servo-control is demonstrated as an effective active compensation method. Nnon-ideal properties of RTD-based temperature sensing are also studied, and digital calibration method is introduced to reduce offset errors in the servo-control.

REFERENCES

[1] Z. Wu, A. Peczalski, V. A. Thakar, Z. Cao, Y. Yuan, G. He, R. L. Peterson, K. Najafi, and M. Rais-Zadeh, "Piezoelectrically transduced high-Q silica micro resonators," *Proc. IEEE MEMS*, Jan. 2013.
[2] Z. Cao, Y. Yuan, G. He, R. L. Peterson, and K. Najafi, "Fabrication of multi-layer vertically stacked fused silica microsystems," *Proc. TRANSDUCERS*, June 2013.
[3] V. A. Thakar, Z. Wu, A. Peczalski, and M. Rais-Zadeh, "Piezoelectrically transduced temperature-compensated flexural-mode silicon resonators," *J. Microelectromechanical Systems*, vol. 22, pp. 815, 2013.
[4] C. M. Jha, M. A. Hopcroft, S. A. Chandorkar, *et al.*, "Thermal isolation of encapsulated MEMS resonators," *J. Microelectromechanical Systems*, vol. 17, pp. 175, 2008.
[5] B. Gilbert, "Translinear circuits: a proposed classification," *Electronics Letters*, vol. 11, pp. 4, 1975.
[6] J. C. Salvia, R. Melamud, S. A. Chandorkar, *et al.*, "Real-Time Temperature Compensation of MEMS Oscillators Using an Integrated Micro-Oven and a Phase-Locked Loop," *J. Microelectromechanical Systems*, vol. 19, pp. 192, 2010.

CONTACT

*Z. Wu, tel: +1-734-389-9507; zzwu@umich.edu